Records of Natural Products

www.acgpubs.org
ORIGINAL ARTICLE

Bioactive compounds from the cultured lichen mycobiont of *Nigrovothelium inspersotropicum*

Y. Thien Vu[1], Thuc-Huy Duong[2], Kiattawee Choowongkomon[3,4], Chanat Aonbangkhen[5], Thi-Thanh-Van Ho[6,7], Hieu-Hien Nguyen[1], Thi-Phuong Nguyen[6,7], Ngoc-Hong Nguyen[8*], Thi-Phi Giao Vo[9], Thi-Hong-Trinh Nguyen[10] and Thi-Minh-Dinh Tran[10*]

[1]Faculty of Pharmacy, Ton Duc Thang University, Ho Chi Minh City, Vietnam
[2]Department of Chemistry, Ho Chi Minh City University of Education, 280 An Duong Vuong Street, Cho Quan Ward, Ho Chi Minh City, 748342, Vietnam
[3]KU Institute for Advanced Studies, Kasetsart University, Bangkok, 10900, Thailand
[4]Department of Biochemistry, Faculty of Science, Kasetsart University, Bangkok, Thailand
[5]Center of Excellence in Natural Products Chemistry, Department of Chemistry, Faculty of Science, Chulalongkorn University, Pathumwan, Bangkok, 10330, Thailand
[6]Center for Hi-Tech Development, Nguyen Tat Thanh University, Saigon Hi-Tech Park, Ho Chi Minh City, Vietnam
[7]NTT Hi-Tech Institute, Nguyen Tat Thanh University, 300A Nguyen Tat Thanh, Xom Chieu Ward, Ho Chi Minh City, Vietnam
[8]CirTech Institute, HUTECH University, 475 A Dien Bien Phu Street, Thanh My Tay Ward, Ho Chi Minh City, Vietnam
[9]Faculty of Biology-Biotechnology, University of Science, Vietnam National University Ho Chi Minh City, Ho Chi Minh City, Vietnam
[10]Department of Biology, Ho Chi Minh City University of Education, 280 An Duong Vuong Street, Cho Quan Ward, Ho Chi Minh City, 748342, Vietnam

Abstract: Cultured lichen mycobionts have been considered as valuable sources of natural compounds with unique structure scaffolds. *Nigrovothelium inspersotropicum*, a crustose lichen from the family Trypetheliaceae, is an indigenous species in Vietnam. However, there is a scarcity of chemical and biological information available regarding *N. inspersotropicum* and its cultured mycobionts. In this study, the mycobiont of *N. inspersotropicum* was cultivated and subjected to chemical and biological investigations. As a result, six compounds, including 3,4-dihydro-7,8-dihydroxy-6-methoxy-3-methylisocoumarin (**1**), (+)-(3*S*)-6,7-dimethoxymellein (**2**), 8-hydroxy-6,7-dimethoxyisocoumarin (**3**), aspermytin A (**4**), subnudatone B (**5**), and *β*-sitosterol (**6**), were isolated and structurally elucidated using extensive spectroscopic analyses (1D- and 2D-NMR and HRESIMS). Notably, compound **1** is new compound, while compound **2** is identified as a new natural compound. The isolated compounds were evaluated for their inhibitory activities against alpha-glucosidase, nitric oxide production, SARS-CoV-2 M^{pro}, and HIV-1 reverse transcriptase. In summary, this study presents new information on natural compounds derived from the mycobiont of *N. inspersotropicum* and their promising anti-inflammatory, antihyperglycemic, and antiviral activities.

Keywords: *Nigrovothelium inspersotropicum*, isocoumarin, alpha-glucosidase inhibition, NO inhibition, HIV-1 reverse transcriptase

Cite this article as:
Vu et al. Bioactive compounds from the cultured lichen mycobiont of *Nigrovothelium inspersotropicum*. (2026). *Records of Natural Products*, 20(4):e25113727

Received: *15 November 2025*
Revised: *07 March 2026*
Accepted: *08 March 2026*
Published: *04 April 2026*

1 Introduction

Lichens represent sophisticated symbiotic consortia, formed by a heterotrophic fungal partner (the mycobiont) and one or more photoautotrophic partners (the photobionts). Functioning as a cohesive biological entity, they are distinguished by their specialized secondary metabolism, which produces a wide range of unique chemical compounds. Many of these lichen-derived metabolites have emerged as high-priority candidates in the search for novel bioactive scaffolds with significant pharmaceutical and biotechnological potential (Rosabal & Pino-Bodas, 2024). Biologically, lichenized fungi form a specialized group that obtain fixed

*Corresponding Authors: Ngoc-Hong Nguyen. Email: nn.hong@hutech.edu.vn; Thi-Minh-Dinh Tran. Email: dinhttm@hcmue.edu.vn

carbon through their photosynthetic partners. While they are ecologically obligate, they exhibit physiological facultativity. Under appropriate *in vitro* conditions, isolated mycobionts can retain metabolic autonomy and grow independently (Yasmin & Jabin, 2024).

This distinct ecological-physiological dichotomy serves as the foundational rationale for their utilization in natural products research. The axenic cultivation of lichen mycobionts effectively separates the fungal partner from the regulatory and metabolic influences of the photobiont. Consequently, laboratory-cultured mycobionts serve as a robust platform for the expression of cryptic biosynthetic gene clusters. Within the field of natural products chemistry, cultured lichen mycobionts are considered valuable sources of unique chemical scaffolds (Duong et al., 2020; Kinoshita et al., 2005; Le et al., 2013, 2024; Miyagawa et al., 1994; Takenaka et al., 2005; Tanahashi et al., 2003; Tran et al., 2024). The compounds isolated from these mycobionts are more closely related to fungal components than to the original lichen (Le et al., 2013). *Nigrovothelium inspersotropicum*, a crustose lichen belonging to the family Trypetheliaceae (Lucking et al., 2016), has not been widely investigated with respect to its chemical constituents. Cultured mycobionts derived from lichens of the family Trypetheliaceae have been comprehensively studied, including genera such as *Trypethelium*, *Marcelaria*, *Astrothelium*, and *Pseudopyrenula* (Duong et al., 2020; Jarupinthusophon et al., 2019; Srinivasan et al., 2020; Sun et al., 2010; Takenaka et al., 2013). These investigations have led to the discovery of novel bioactive compounds from cultured mycobionts. For example, subnudatones A and B were isolated from *Pseudopyrenula subnudata*, with subnudatone A showing moderate cytotoxicity against K562 and MCF-7 cell lines (IC_{50} 23.5 ± 1.0 and 51.9 ± 1.4 μM, respectively). From the cultured mycobiont of *Marcelaria cumingii*, several trypethelone derivatives were identified, including (–)-2′ *S*-trypethelone methyl ether, which exhibited selective inhibition of HCT116 and A549 cells (IC_{50} 0.32 ± 0.03 and 1.05 ± 0.12 μM, respectively). Additional new trypethelones, along with naphthoquinone and phenalenone derivatives, have been isolated from cultured mycobionts of *Trypethelium eluteriae* and *Trypethelium* sp.. Similarly, 7-hydroxy-8-methoxytrypethelone from *Astrothelium* sp. displayed modest antibacterial activity against *Enterococcus faecalis* and methicillin-resistant *Staphylococcus aureus*. Collectively, these findings underscore the remarkable biosynthetic capacity of the Trypetheliaceae family and highlight its strong potential as a reservoir of novel therapeutic scaffolds, suggesting that unexplored members may yield additional valuable secondary metabolites. However, there is limited information regarding the chemical profiles of *N. inspersotropicum* and its cultured mycobionts both in terms of their biological and chemical properties. Recent investigations of the genus *Nigrovothelium* have mainly focused on its taxonomy (Aptroot & Lücking, 2016; Gogoi et al., 2022; Lucking et al., 2016; Satapathy et al., 2021; Singh et al., 2018). These studies indicated that the mentioned lichen has been distributed in Brazil, India, and Vietnam. In the ongoing research on Vietnamese lichen mycobionts (Duong et al., 2020; Le et al., 2013, 2024; Tran et al., 2024), the mycobiont of *N. inspersotropicum* was successfully cultivated and chemically analyzed. The primary objective of this research is to investigate the chemical and biological data of the mycobiont of *N. inspersotropicum*, with a specific focus on the inhibition of alpha-glucosidase and nitric oxide (NO), and the inhibition of the HIV virus and SARS-CoV-2 M^{pro}. In summary, this study presents novel insights into natural compounds extracted from the mycobiont of *N. inspersotropicum*, highlighting their potential anti-inflammatory, antihyperglycemic, and antiviral activities.

2 Materials and Methods

2.1 General Experimental Procedures

NMR spectra were obtained on a Bruker Avance III instrument operating at 500 MHz for ^{1}H and 125 MHz for ^{13}C, with tetramethylsilane (TMS) used as the internal reference. High-resolution electrospray ionization mass spectrometric (HRESIMS) data were acquired on a MicrOTOF–Q system coupled to an Agilent 1100 LC–MSD Trap platform. Thin-layer chromatography (TLC) was performed on Merck precoated silica gel plates (60 F254 or RP-18 F254S), and the chromatographic spots were detected by spraying with 10% H_2SO_4 followed by heating. Open-column chromatography was conducted using silica gel 60 (particle size 0.040–0.063 mM, Himedia). *Saccharomyces cerevisiae* α-glucosidase (E.C. 3.2.1.20) and acarbose used in the enzyme assays were purchased from Sigma-Aldrich.

2.2 Lichen Material and Mycobiont Culture

The lichen *N. inspersotropicum* was collected from the bark of trees in Long An Province (10.769665, 105.940201), Vietnam in May 2022. The voucher specimens (registration PHH0011357) were identified by Dr. Vo Thi Phi Giao, University of Science and deposited at University of Sciences, Ho Chi Minh City, Vietnam.

The method of mycobiont culture followed that presented in the former reports (Do et al., 2022a; Tran et al., 2024) with slight modifications. The procedure began by cleaning the lichen sample under tap water for 15 min to remove adhering debris. The next step involved surface disinfection via a 90-second soak in 70% ethanol, after which the sample was rinsed three separate times in sterile distilled water. After rinsing, the sample was placed in a clean bench for natural drying. Thin sections of the lichen thallus were prepared using a sterile razor blade and mounted on slides to visualize fungal spores under 4x and 10x objectives. Spores were then collected using a micropipette and inoculated onto Petri dishes containing MY10 medium (10 g/L malt extract, 4 g/L yeast extract, 100 g/L sucrose, and 15 g/L agar). Subsequently, the cultures were incubated in darkness at 18°C. The plates were monitored at weekly intervals to observe the emergence of mycobiont colonies. Plates showing pure mycobiont growth were then transferred to 22°C for an additional two months to achieve sufficient biomass. Subsequently, the colonies were cut into small pieces using a sterile scalpel, and the resulting fragments were transferred onto fresh MY10

http://doi.org/10.25135/rnp.2511.3727
Rec. Nat. Prod. 2026, 20(4):e25113727

medium. These subcultures were then incubated in the dark at 22°C for three months.

The lichen mycobiont's voucher specimen (No. UE-MY05) was stored at Department of Biology, Ho Chi Minh City University of Education.

2.3 Extraction and Isolation

The harvested colonies (60 g dry weight) were ground into a fine powder and subsequently macerated with ethyl acetate (10 × 800 mL, weekly intervals). The combined extracts were concentrated under reduced pressure to yield 2.5 g of crude EtOAc extract. This extract was subjected to silica gel column chromatography (CC) and eluted with an *n*-hexane–EtOAc gradient (10:1 to 0:10, v/v), resulting in six fractions: EA1 (301 mg), EA2 (450 mg), EA3 (420 mg), EA4 (435 mg), EA5 (360 mg), and EA6 (500 mg).

Specifically, fraction EA1 was further purified by silica gel CC, eluting with *n*-hexane: $CHCl_3$ (1:1, v/v) to afford three sub-fractions: EA1.1 (52 mg), EA1.2 (46 mg), and EA1.3 (105 mg). Fraction EA1.3 was then subjected to C_{18} reverse-phase silica gel chromatography using methanol:water (5:1, v/v) as the eluent, yielding compounds **5** (2.5 mg) and **6** (30.0 mg).

Fraction EA3 was fractionated via silica gel CC using a gradient of *n*-hexane:EtOAc:acetone (10:1:1 to 0:1:1, v/v/v), yielding four sub-fractions: EA3.1 (85 mg), EA3.2 (150 mg), EA3.3 (70 mg), and EA3.4 (110 mg). Fraction EA3.1 was further chromatographed over silica gel and eluted with $CHCl_3$: acetone (10:1, v/v) to obtain compound **3** (2.5 mg). Fraction EA3.4 was purified by silica gel CC with a mobile phase of *n*-hexane: $CHCl_3$: EtOAc: acetone (5:1:0.5:0.5, v/v/v/v) to give compounds **1** (1.7 mg) and **2** (2.1 mg).

Finally, fraction EA4 was subjected to silica gel CC, eluted with *n*-hexane: $CHCl_3$: EtOAc: acetone (5:1:2:2, v/v/v/v), providing three sub-fractions: EA4.1 (125 mg), EA4.2 (50 mg), and EA4.3 (200 mg). Compound **4** (5.0 mg) was purified from fraction EA4.1 using silica gel CC eluted with $CHCl_3$: acetone (9:1, v/v).

2.4 Alpha-Glucosidase Inhibition

The α-glucosidase enzyme inhibition assay followed the protocol described by Do et al. (2022b). The samples were diluted in a phosphate buffer (0.1 M, pH 6.9), which also contained 5% DMSO. The α-glucosidase enzyme (0.1 U/mL) and p-nitrophenyl-α-D-glucopyranoside substrate (5 mM) were prepared in a phosphate buffer (0.1 M, pH 6.9). Each well of a 96-well plate received 50 µL of the sample (in triplicate) followed by 40 µL of the enzyme solution. Control wells were prepared by substituting the sample with a 5% DMSO solution. The plate was incubated at 37°C for 20 minutes. Next, 40 µL of the substrate solution was added to each well, and the incubation continued at 37°C for an additional 20 min. The reaction was terminated by adding 130 µL of 0.2 M Na_2CO_3 to the mixture. The absorbance of the mixture was measured at 405 nanometers using a CLARIOstar Plus multimode microplate reader (BMG LABTECH, Ortenberg, Germany). The percentage of inhibition of α-glucosidase activity was evaluated using the following formula:

$$\alpha\text{-Glucosidase inhibition percentage (\%)} = \left(1 - \frac{OD\ of\ sample}{OD\ of\ control} \times 100\right)$$

2.5 HIV-1 Reverse Transcriptase Inhibition

A 2.5 µL aliquot of Poly(A) ribonucleotide template (at a concentration of 1 mg/mL) and a 2.5 µL aliquot of Oligo d(T)16 primer (at a concentration of 50 µg/mL) were hybridized in a sterile tube to gain the mixture **X**. The mixture was incubated at ambient temperature for 60 minutes to allow annealing. Subsequently, 1 mL of a polymerization buffer including Tris-HCl (60 mM, pH 8.1), potassium chloride (60 mM), magnesium chloride (8 mM), DTT (13 mM), and dTTP (100 µM) was added to the tube. The assay to identify compounds capable of inhibiting HIV-1 reverse transcriptase was conducted in a 96-well black plate. Initially, the 3 µL volume of a reaction buffer (20 mM Tris at pH 7.5, 100 mM NaCl, 2 mM DTT, and 0.4 mM EDTA) was added to each well. Subsequently, 15 µL of the mixture **X** was added to each well. The compounds were dissolved in dimethyl sulfoxide and subsequently added to the reaction mixture to attain a final concentration of 10 µM. The mixture was incubated at room temperature for 30 minutes following the addition of 5 µL of 25 nM HIV-1 reverse transcriptase. The reaction was terminated by adding 2 µL of 0.2 M EDTA. Subsequently, 173 µL of PicoGreen dye dissolved in 1X Tris-EDTA buffer was added to the reaction mixture. The fluorescence intensity of the reaction mixture was immediately quantified in endpoint mode at 485 nM for excitation and 535 nM for emission using an Infinite 200 Pro multimode microplate reader (Tecan, USA). A reaction without any inhibitor served as the control. For the blank, the inhibitor was replaced with DMSO, and EDTA was added before the enzyme. Nevirapine at 1 µM was used as a positive control. The inhibition percentage was calculated as the following equation: $\%I = \left(1 - \frac{Fs\text{-}Fb}{Fc\text{-}Fb}\right) * 100$, where Fs: fluorescence intensity of the samples, Fc: fluorrescence intensity of control, Fb: fluorrescence intensity of blank (Tran et al., 2024).

2.6. Molecular Docking Study of Anti-Inflammatory Activity of 1

The phosphodiesterase 4 (PDE4) protein was obtained from the Protein Bank (PDB: 4WCU), then *in silico* studies were performed using Schrodinger software. The protein was first prepared using Protein Preparation Wizard (Madhavi Sastry et al., 2013), then water was removed from the structure, binding site were created using Receptor Grid Generation. Ligands were prepared using Ligprep. The docking process included Glide Docking which consisted of 2 steps: Standard precision (SP) and Extra precision (XP) and finally MM-GBSA (Jacobson et al., 2004) calculation.

2.7 Nitric Oxide Inhibition

The inhibition of nitric oxide production by compounds **1–6** was determined with the same procedure previously reported

(Ngoc Mai et al., 2024; Sukandar et al., 2023). RAW264.7 cells were initially seeded into 96-well plates at a density of 6×10^4 cells per well and cultured for 24 h. Subsequently, the cells were exposed to 100 ng/mL lipopolysaccharides (LPS) either alone (as a control) or in the presence of the test compounds at concentrations of 50 and 100 µM for 24 h at 37°C. To quantify nitric oxide production, 100 µL of the culture supernatant was mixed with an equal volume of Griess reagent (Sigma-Aldrich, G4410) and incubated at room temperature for 10 min. The absorbance was then recorded at 540 nM using a Thermo Scientific Varioskan LUX microplate reader. Each sample underwent triplicate analysis at five distinct concentrations that were positioned around the IC_{50} value. The mean values obtained from these analyses were recorded. L-NMMA served as a positive control.

2.8. SARS-CoV-2 M^{pro} Inhibition

A Fluorescence Resonance Energy Transfer (FRET)–based assay was used to assess the inhibitory activity of the test compounds against SARS-CoV-2 Mpro. Working solutions of the protease and the fluorogenic substrate were prepared in buffer X (20 mM Tris, pH 7.5, 100 mM NaCl, 2 mM DTT, and 0.4 mM EDTA), whereas buffer Y, which lacked DTT, was employed for diluting the test samples. All reactions were set up in a black 384-well microplate with a final assay volume of 25 µL per well. Each reaction began with the addition of 10 µL of buffer X, followed by 5 µL of SARS-CoV-2 Mpro (3 µM). Test compounds were then introduced to achieve a final concentration of 10 µM. After a 10-min incubation at room temperature, the FRET substrate was added to reach 40 µM. Fluorescence was continuously monitored for 30 min at 1-min intervals on an Infinite 200 Pro multimode plate reader (Tecan, USA) using excitation at 340 nM and emission at 430 nM. The SARS-CoV-2 M^{pro} inhibition percentage of compounds was determined using the following equation: $\%I = (1 - [S_S/S_c]) * 100$, where S_S is the slope of the reaction with inhibitor, S_c is the slope of the reaction without inhibitor, and S_b is the enzymatic blank. A series of ten concentrations, ranging from 80 µM to 0.2 µM, were prepared through twofold serial dilutions for the determination of the IC_{50} values of the compounds. For IC_{50} determination, ten serial twofold dilutions (0.2–80 µM) of each compound were prepared. Dose–response curves were generated using GraphPad Prism 8.0.1 (GraphPad Software, USA), and IC_{50} values were obtained by nonlinear regression using a variable-slope model.

2.9 Statistical Analysis

Three independent experiments were conducted to evaluate NO inhibitory and cytotoxic activities, as well as alpha-glucosidase inhibitory activity. Data are presented as mean ± standard deviation. Statistical analysis between samples was performed using ANOVA for alpha-glucosidase inhibitory activity.

3 Results and Discussion

The lichen *N. inspersotropicum* was collected from the bark of *Hopea* trees. The lichen was stored in a cold environment, and its mycobiont component was subsequently isolated. The mycobiont was subsequently cultivated under controlled conditions for two months. The resulting biomass was collected and further utilized for chemical analyses. The crude EtOAc extract of the mycobiont was prepared and subsequently subjected to various isolation techniques (Scheme 1), yielding eight compounds **1–6**: 3,4-dihydro-7,8-dihydroxy-6-methoxy-3-methylisocoumarin (**1**), (+)-(3*S*)-6,7-dimethoxymellein (**2**) (Choudhary et al., 2004), 8-hydroxy-6,7-dimethoxyisocoumarin (**3**) (Kiang et al., 1994), aspermytin A (**4**) (Tsukamoto et al., 2004a), subnudatone B (**5**) (Duong et al., 2020), and *β*-sitosterol (**6**) (Figure 1). The structures of these compounds were determined by extensive spectroscopic analyses (1D- and 2D-NMR and HRESIMS). The structural elucidation of these compounds was described as follows.

The molecular formula of **1** was determined as $C_{12}H_{14}O_6$ based on a protonated ion peak at *m/z* 255.0854 $[M + H]^+$ (calc. for $C_{12}H_{15}O_6$, 255.0863) in the HR-ESI-MS mass spectrum. The ^{1}H NMR spectrum in chloroform-d_1 showed one proton aromatic [δ_H 6.55 (1H, *s*, H-5)], two methoxy groups [δ_H 3.96 (3H, *s*, 6-OCH_3) and δ_H 3.91 (3H, *s*, 7-OCH_3)], one hydrogen-bonded hydroxy group [δ_H 11.16 (1H, *s*, 8-OH)], one *doublet* methyl [δ_H 1.58 (3H, *d*, *J* = 6.8 Hz, H-3′)], and two oxymethines [δ_H 4.65 (1H, *qd*, *J* = 6.8, 2.5 Hz, H-3) and 4.50 (1H, *dd*, *J* = 6.8, 1.8 Hz, H-4)]. The ^{13}C-NMR spectrum, in conjunction with the HSQC and HMBC data, revealed four quaternary carbons [δ_C 159.1 (C-6), 156.6 (C-8), 137.4 (C-7), 136.6 (C-4a), and 117.4 (C-8a)], three methine carbons [δ_C 102.9 (C-5), 78.1 (C-3), 67.7 (C-4)], two methoxy carbons [δ_C 60.8 (7-OCH_3), 56.5 (6-OCH_3)], and one methyl carbon [δ_C 16.0 (C-3′)]. In the A-ring, the positions of two methoxy groups [δ_H 3.96 (3H, *s*, 6-OCH_3) and 3.91 (3H, *s*, 7-OCH_3)] were determined by HMBC correlations of H-5 (δ_H 6.55) to three quaternary carbons at δ_C 159.1 (C-6) and 137.4 (C-7); of 6-OCH_3 (δ_H 3.96) to C-6; and 7-OCH_3 (δ_H 3.91) and C-7, and of 8-OH [δ_H 11.16 (1H, *s*)] to C-7 and C-8 (Figure 2). In the B-ring, HMBC correlations of the methyl H_3-3′ (δ_H 1.58) and two methine carbons at δ_C 78.1 (C-3) and 67.7 (C-4) indicated the spin system through C-3 and C-4. The relative configuration of **1** was determined as a *trans* configuration of H-3 and H-4, defined by the coupling constant $J_{H\text{-}3/H\text{-}4}$ being 6.8 Hz that was evidently observed in the ^{1}H NMR spectrum in acetone-d_6 (see Supporting information), similar to that of related compounds (Ayer et al., 1993; Duan et al., 2018; He et al., 2016; Yang et al., 2011). This finding was strongly supported by a key NOESY correlation between H_3-3′ and H-4. A comparison of the NMR data of **1** with lignicol (Ayer et al., 1993) and (3*R*,4*R*)-6,7-dimethoxy-4-hydroxymellein (Choudhary et al., 2004) revealed notable similarities (Table S1). In conjunction with these findings, the chemical structure of compound **1** was elucidated and subsequently named nigrovothelone, as depicted in Figure 1.

http://doi.org/10.25135/rnp.2511.3727
Rec. Nat. Prod. 2026, 20(4):e25113727

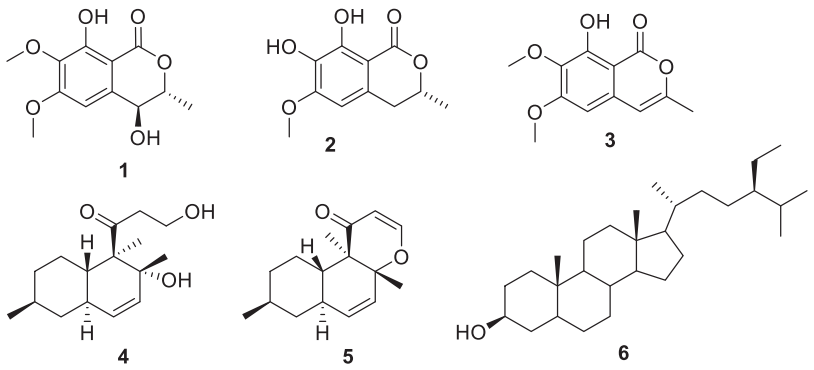

Figure 1. Chemical structures of compounds **1–6**

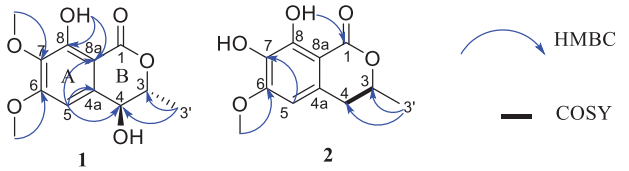

Figure 2. HMBC and COSY correlations of **1–2**

The 1D and 2D NMR spectra of compound **2** exhibited striking similarities to those of compound **1** (Table 1), suggesting a structural relationship. The chemical structure of compound **2** was subsequently determined to be 3,4-dihydro-7,8-dihydroxy-6-methoxy-3-methylisocoumarin, a previously identified compound (Ayer et al., 1993; Duan et al., 2018; Mali et al., 1993, p. 1). Mali and colleagues synthesized a mixture of two enantiomers of **2** (Mali et al., 1993).

Table 1. ^{1}H-NMR (500 MHz, *J* in Hz) and ^{13}C-NMR (125 MHz) of **1–2**

No	1		2	
	δ_H[a]	δ_C[a]	δ_H[b]	δ_C[b]
1		169.0		171.7
3	4.65 (*qd*, 6.8, 2.5)	78.1	4.50 (*m*)	73.7
4	4.50 (*dd*, 6.8, 1.8)	67.6	2.88 (*m*)	33.2
4a		130.2*		133.9
5	6.55 (*s*)	102.8	6.57 (*s*)	111.2
6		156.6*		157.3
7		137.8*		127.8
8		154.4*		156.8
8a		121.3*		126.0
3′	1.58 (*d*, 6.8)	16.0	1.48 (*d*, 6.0)	20.5
4-OH				
6-OMe	3.96 (*s*)	56.2	3.92 (*s*)	56.0
7-OMe	3.91 (*s*)	60.8		
8-OH	11.16 (*s*)		15.28 (*s*)	

Note: Recorded in [a]chloroform-d_1 [b]DMSO-d_6 *determined by HMBC correlations.

However, the 1D NMR data for this mixture was incomplete. Consequently, compound **2** was identified as a new natural compound.

The absolute configuration of **1** and **2** were determined from ECD data (Figure 3), which exhibited strong negative Cotton effects at 270–275 nM (Ayer et al., 1993; Duan et al., 2018). This indicated that **1** and **2** have a 3*R* configuration and further defined a 4*S* configuration of **1**.

Compounds **1–3** belong to the isocoumarin class, a group of metabolites renowned for their diverse pharmacological profiles (Tammam et al., 2023). As noted by Cai et al. (2022), isocoumarins isolated from the mangrove-derived fungus *Talaromyces flavus* exhibited potent antioxidant and α-glucosidase inhibitory activities superior to standard controls, highlighting their potential as therapeutic agents for oxidative stress and diabetes management (Cai et al., 2022). The class of dihydroisocoumarins represents a significant group of naturally occurring lactones that continue to attract interest due to their diverse biological activities and structural diversity. Recent literature highlights their potential as multi-target bioactive agents, particularly in anti-inflammatory, antioxidant, cytotoxic, and enzyme inhibitory contexts (Ortiz et al., 2019). For example, secondary metabolites belonging to dihydroisocoumarins have been reported to exhibit anti-inflammatory effects by modulating pro-inflammatory mediators, suggesting therapeutic relevance for chronic inflammatory disorders (Sun et al., 2025).

Sun and colleagues demonstrated that the specific rotation of aspermytin A was determined to have opposite signs in acetonitrile (ACN) and chloroform (Sun et al., 2017). Notably, no ECD data for aspermytin A has been discovered (Inoue, 2010; Inoue et al., 2013). Tsukamoto and co-workers determined the absolute configuration of (+)-aspermytin A using ECD data of its structural analog (Figure 4) (Tsukamoto et al., 2004b). The CE values of compound **4**, including a positive CE at 230 nM, a negative CE at 250 nM, and a positive CE at 310 nM, were consistent with those of peaurantiogriseol A (Ma et al., 2015). Compound **5** was elucidated as subnudatone B, previously isolated by Duong and co-workers (Duong et al., 2020). The relative configuration of this compound was defined using the NOESY spectrum and comparison with NMR data recorded in the same chloroform-*d*. However, the absolute configuration of **5** has not been determined yet. The

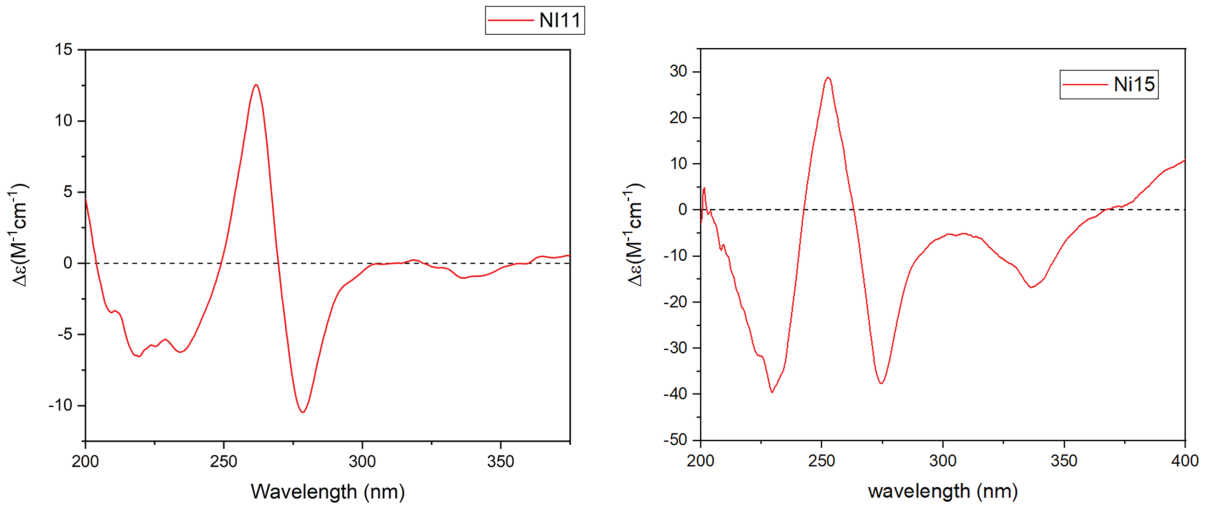

Figure 3. ECD data of **1** (left) and **2** (right)

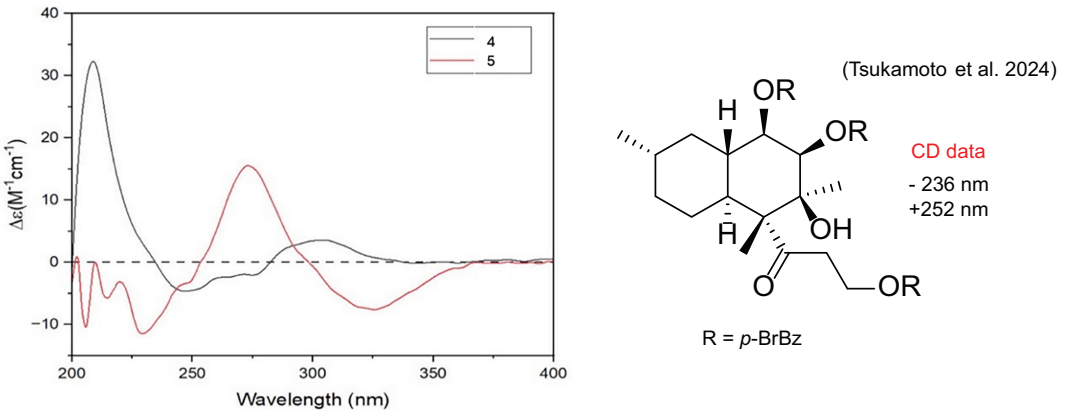

Figure 4. ECD spectra of **4**–**5**

opposite CEs at 250–260 nM and 310–320 nM for **4** and **5** (Figure 4) indicated they had opposite configurations of C-4, C-10, and C-14.

(+)-Aspermytin A (**4**) exhibited significant neurotrophic effect on the rat pheochromocytoma cells (PC-12) (Tsukamoto et al., 2004a) but the enantiomer (–)-Aspermytin A showed no activity of inducing neurite outgrowth and antimicrobial activity against *Escherichia coli* (ATCC 25922), *Staphylococcus aureus* (ATCC 25923), and *Candida albicans* (ATCC 60193). (+)-Aspermytin A showed the inhibition against the proliferation of $CD3^+$ T cells (Sun et al., 2017). Little is known about the biological activity of **1–5**.

3.1 Alpha-Glucosidase Inhibition

The compounds **1–6** were assessed for their potential to inhibit *α*-glucosidase. While most of them did not demonstrate significant inhibitory activity, compound **6** showed a moderate level of inhibition, with IC_{50} of 132.3 ± 7.7 μg/mL (Figure 5). This value is lower than that of acarbose (IC_{50} = 203.9 ± 11.0 μg/mL), suggesting that compound **6** has a stronger inhibitory effect compared to the reference standard.

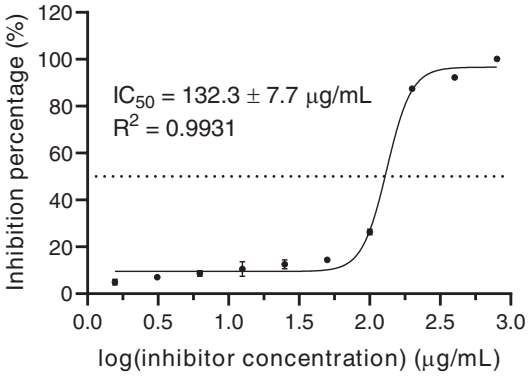

Figure 5. Dose-response curve for the alpha-glucosidase inhibition by **6**

3.2 NO Inhibitory Activity

Compounds **1–6** were evaluated for their inhibitory activity on nitric oxide (NO) production in LPS-induced RAW 264.7 macrophage cells, using L-NMMA (IC_{50} 41.3 μM) as the positive control (Table 2). As shown in Table 2, compound

http://doi.org/10.25135/rnp.2511.3727
Rec. Nat. Prod. 2026, 20(4):e25113727

Table 2. NO production inhibitory effect of **1–6**

Compounds	NO inhibition IC_{50} (μM)[a]	Cytotoxicity in RAW 264.7 cells IC_{50} (μM)[a]
1	7.18 ± 0.25	>100
2	>100	>100
3	>100	>100
4	>100	>100
5	>100	>100
6	>100	>100
L-NMMA[b]	41.3 ± 3.6	>100

Note: [a]Data presented as mean ± standard deviation (SD). [b]Positive control.

Table 3. SARS-CoV-2 M^{pro} inhibition of compounds

Compounds	Inhibition percentage (%)
1	0.16 ± 0.06
2	0.60 ± 0.02
3	8.67 ± 0.06
4	1.92 ± 0.34
5	1.3 ± 0.07
6	56.0 ± 0.50
Lopinavir (1 μM)	33.46 ± 0.69

1 exhibited notable NO inhibitory activity, with IC_{50} values of 7.18 ± 0.25 μM. Both compounds were more potent than the positive control, L-NMMA. In contrast, compounds **2–6** showed no significant inhibition of NO production. Importantly, none of the compounds exhibited cytotoxicity at concentration up to 100 μM, suggesting that the inhibition of NO production observed was not a result of general cytotoxicity but was instead due to specific inhibitory mechanisms targeting NO synthesis.

3.3 SARS-CoV-2 M^{pro} Inhibition

Compounds **1–2** and **5–6** were screened for SARS-CoV-2 M^{pro} inhibition at a final concentration of 10 μM. The highest activity was observed for compound **6**, with inhibition percentages of 56.0% (Table 3). IC_{50} value of compound **6** was determined to be 6.50 ± 0.44 μM (Figure 6), lower than that of lopinavir (122.5 μM), suggesting a stronger inhibitory activity. In contrast, compounds **1**, **2**, and **5** exhibited negligible inhibitory activity, with inhibition percentages of 0.16%, 0.60%, and 1.3%, respectively. These findings suggest that the structural features of compound **6** may contribute to their higher affinity for the SARS-CoV-2 M^{pro} active site, making them potential candidates for further optimization.

3.4 HIV-1 Reverse Transcriptase Inhibition

Compounds **1–2**, and **6** were assessed for their inhibitory capacity against HIV-1 reverse transcriptase at a final concentration of 200 μM (Table 4). Among these compounds, compound **7** exhibited no inhibitory activity. Compound **2** demonstrated weak inhibition of HIV-1 reverse transcriptase,

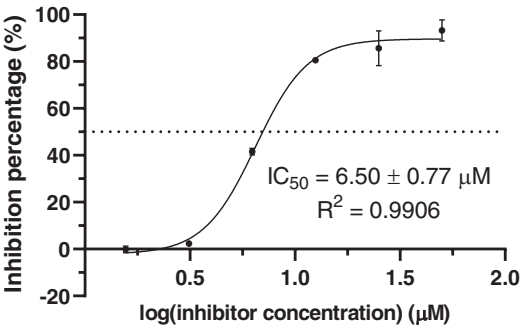

Figure 6. Dose-response curve for the M^{pro} inhibition by **6**

Table 4. HIV-1 reverse transcriptase inhibition by compounds

Compound	Inhibition percentage (%)
1	53.5 ± 0.3
2	32.5 ± 0.1
3	1.2 ± 0.1
4	4.2 ± 0.1
5	20.7 ± 0.3
6	0.2 ± 0.1
Nevirapine (1 μM)	38.3 ± 2.5

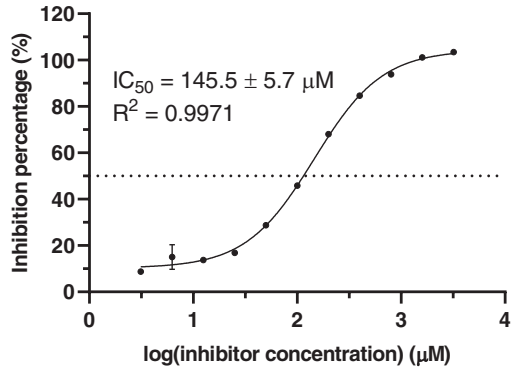

Figure 7. Dose-response curve for inhibition of HIV-1 reverse transcriptase by **1**

approximately 30%, while compound **1** displayed the most potent inhibitory effect, with a 53.5% inhibition rate. The IC_{50} value for compound **1** was determined to be 145.5 ± 5.7 μM (Figure 7), indicating moderate activity. This value is higher than that of Nevirapine (1.6 ± 0.1 μM), suggesting that compound **1** exhibits weaker activity in comparison. These results suggest that the chemical structure of compound **1** may be more suitable for interaction with the reverse transcriptase enzyme than the other compounds tested, making it a promising candidate for further optimization as an HIV-1 reverse transcriptase inhibitor.

Table 5. The substantial ligand interactions between the optimal docking pose and the receptor 4WCU

Compounds	Docking score	MM-GBSA (kcal/mol)	Interaction
Native ligand	−10.0	−83.4	Pi-pi stacking: Phe 372 H-bond: Hip 160, Met 273, Gln 433
1	−8.5	−59.9	Pi-pi stacking: Phe 372 H-bond: Asn 321, Gln 369

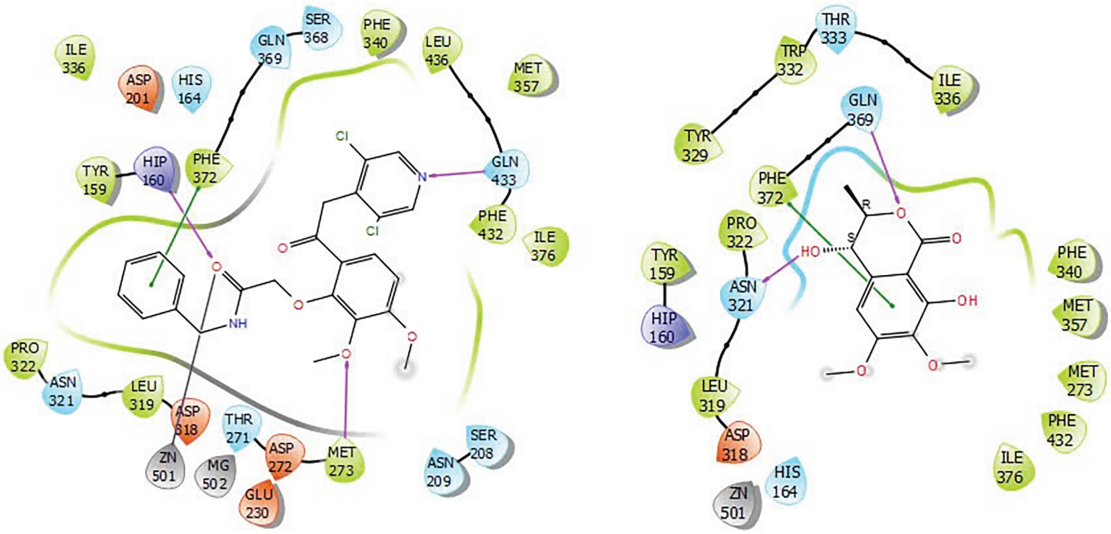

Native ligand **1**

Figure 8. The 2D diagram of interactions between **1** and **4** WCU

3.5 Molecular Docking of Anti-Inflammatory Activity of 1

The results indicated that the pi-pi stacking interaction between Phe372 facilitated the stabilization of the directional core of both the native ligand and the two studied ligands. However, hydrogen bonding interactions were not replicated between the native ligand and the two studied ligands due to substantial differences in size (with the native ligand being larger) and the varying substituents attached to the molecules (Figure 8). The docking scores revealed that the native ligand had a superior pose score of −10 kcal/mol, compared to −8.5 kcal/mol for ligand **1** (Table 5). This difference translated into a proportional binding affinity to the protein, with the two studied ligands exhibiting only approximately 70–80% of the binding affinity with the reference ligand (−59.9 kcal/mol of ligand **1** compared to −83.4 kcal/mol of native ligand).

4 Conclusions

From the cultured mycobiont of the lichen *N. inspersotropicum*, six compounds nigrovothelone (**1**), 3,4-dihydro-7,8-dihydroxy-6-methoxy-3-methylisocoumarin (**2**), 8-hydroxy-6,7-dimethoxyisocoumarin (**3**), aspermytin A (**4**), subnudatone B (**5**), and β-sitosterol (**6**), were isolated and structurally elucidated. Notably, compounds **1–2** are new natural compounds. Among these compounds, **1** exhibits substantial nitric oxide inhibitory activity in both *in vitro* and *in silico* assays, suggesting their potential as anti-inflammatory agents. Compound **1** exhibited moderate HIV-1 reverse transcriptase inhibition with an IC_{50} value of 145.5 ± 5.7 μM, indicating potential antiviral properties. Compound **6** showed moderate alpha-glucosidase inhibition, suggesting a possible role in managing hyperglycemia.

Funding Statement

This research is funded by Ministry of Education and Training under grant number B2024-SPS-05.

Author Contributions

Conceptualization, T.H.D, T.M.D.T, N.H.N; methodology, T.M.D.T, N.H.N, K.C; software, C.A, K.C; formal analysis, H.H.N, T.P.N, T.M.D.T; investigation, Y.T.V, T.M.D.T, T.H.D; resources, H.H.N, T.P.N, T.P.G.V; data curation, T.H.T.N, C.A; writing-original draft preparation, Y.T.V, T.H.D, T.M.D.T, N.H.N.; writing-review and editing, all authors. All authors have read and agreed to the published version of the manuscript.

Availability of Data and Materials

The authors declare that the data supporting the findings of this study are available within the paper and its Supplementary Information files. Should any raw data files be needed in another format they are available from the corresponding author upon reasonable request. Source data are provided with this paper.

Conflicts of Interest

The authors declare that they do not have any conflict of interest.

Supporting Information

Supporting information accompanies this paper on http://www.acgpubs.org/journal/records-of-natural-products.

ORCID

Y Thien Vu: 0000-0003-1210-7246
Thuc-Huy Duong: 0000-0001-9891-4326
Kiattawee Choowongkomon: 0000-0002-2421-7859
Chanat Aobangkhen: 0000-0002-7378-1341
Thi-Thanh-Van Ho: 0000-0002-3898-4709
Hieu-Hien Nguyen: 0009-0009-5418-6123
Thi-Phuong Nguyen: 0000-0002-6406-1406
Ngoc-Hong Nguyen: 0000-0002-3119-1802
Thi-Phi Giao Vo: 0000-0002-7807-3360
Thi-Hong-Trinh Nguyen: 0009-0000-7606-5490
Thi-Minh-Dinh Tran: 0009-0005-3976-0570

References

Aptroot, A. & Lücking, R. (2016). A revisionary synopsis of the *Trypetheliaceae* (Ascomycota: *Trypetheliales*). *The Lichenologist*, *48*(6), 763–982. DOI: 10.1017/S0024282916000487.

Ayer, W., Lu, P., Orszanska, H. & Sigler, L. (1993). Deoxyscytalidin and lignicol: New metabolites from scytalidium species. *Journal of Natural Products*, *56*(10), 1835–1838. DOI: 10.1021/np50100a029.

Cai, J., Zhu, X.-C., Zeng, W.-N., Wang, B., Luo, Y.-P., Liu, J., Chen, M.-J., Li, G.-Y., Huang, G.-L., Chen, G.-Y., Xu, J. & Zheng, C.-J. (2022). Talaromarins A-F: Six new isocoumarins from mangrove-derived fungus *Talaromyces flavus* TGGP35. *Marine Drugs*, *20*(6), 361. DOI: 10.3390/md20060361.

Choudhary, M. I., Musharraf, S. G., Mukhmoor, T., Shaheen, F. & Ali, S. (2004). Isolation of bioactive compounds from aspergillus terreus. *Zeitschrift für Naturforschung B*, *59*(3), 324–328. DOI: 10.1515/znb-2004-0315.

Do, T.-H., Aree, T., Nguyen, H.-H., Nguyen, H.-C., Vo, T.-P. G., Nguyen, N.-H. & Duong, T.-H. (2022a). Two new guaiane-sesquiterpenes from the cultured lichen mycobiont of *Diorygma pruinosum*. *Phytochemistry Letters*, *52*, 59–62. DOI: 10.1016/j.phytol.2022.09.005.

Do, T.-H., Duong, T.-H., Nguyen, H. T., Nguyen, T.-H., Sichaem, J., Nguyen, C. H., Nguyen, H.-H. & Long, N. P. (2022b). Biological activities of lichen-derived monoaromatic compounds. *Molecules*, *27*(9), 2871. DOI: 10.3390/molecules27092871.

Duan, Y.-Q., Dang, L.-Z., Jiang, J.-X., Zhang, Y.-P., Xiang, N.-J., Yang, H.-M., Du, G., Yang, H.-Y. & Li, Q.-Q. (2018). Anti-tobacco Mosaic virus isocoumarins from the fermentation products. *Chemistry of Natural Compounds*, *54*, 249–252.

Duong, T.-H., Nguyen, H.-H., Le, T.-T., Tran, T.-N., Sichaem, J., Nguyen, T.-T., Nguyen, T.-P., Mai, D.-T., Nguyen, H.-H. & Le, H.-D. (2020). Subnudatones A and B, new trans-decalin polyketides from the cultured lichen mycobionts of *Pseudopyrenula subnudata*. *Fitoterapia*, *142*, 104512. DOI: 10.1016/j.fitote.2020.104512.

Gogoi, R., Devi, D., Nayaka, S. & Yasmin, F. (2022). A checklist of lichens of Assam, India. *Asian Journal of Conservation Biology*, *11*(1), 49–65. DOI: 10.53562/ajcb.73760.

He, J.-W., Xu, H.-S., Yang, L., He, W.-W., Wang, C.-X., Lin, F., Lian, Y.-Y., Sun, B.-H. & Zhong, G.-Y. (2016). New isocoumarins and related metabolites from *Talaromyces flavus*. *Natural Product Communications*, *11*(6), 805–807. DOI: 10.1177/1934578x1601100627.

Inoue, A. (2010). Total synthesis of (+)-aspermytin A. *Tetrahedron Letters*, *51*(30), 3966–3968. DOI: 10.1016/j.tetlet.2010.05.107.

Inoue, A., Mori, S., Yoshida, M. & Shishido, K. (2013). An efficient access to Aspermytin A and Oblongolide C through an intra-molecular nitrile oxide-alkene [3+2] cycloaddition. *Synlett*, *24*(01), 61–64. DOI: 10.1055/s-0032-1317693.

Jacobson, M. P., Pincus, D. L., Rapp, C. S., Day, T. J. F., Honig, B., Shaw, D. E. & Friesner, R. A. (2004). A hierarchical approach to all-atom protein loop prediction. *Proteins: Structure, Function, and Bioinformatics*, *55*(2), 351–367. DOI: 10.1002/prot.10613.

Jarupinthusophon, S., Luangsuphabool, T., Aree, T., Duong, T.-H., Lugsanangarm, K., Onsrisawat, P., Siripong, P., Sangvichien, E. & Chavasiri, W. (2019). Naphthoquinones from cultured Mycobiont of *Marcelaria cumingii* (Mont.) and their cytotoxicity. *Natural Product Communications*, *14*(12), 1934578X19884383. DOI: 10.1177/1934578X19884383.

Kiang, F. M., Chang, S. J. & Wu, C. L. (1994). Naphthalene and isocoumarin derivatives from the liverwort Wettsteinia inversa. *Phytochemistry*, *37*(5), 1459–1461. DOI: 10.1016/s0031-9422(00)90433-3.

Kinoshita, K., Yamamoto, Y., Takatori, K., Koyama, K., Takahashi, K., Kawai, K. & Yoshimura, I. (2005). Fluorescent compounds from the cultured Mycobiont of Amygdalaria panaeola. *Journal of Natural Products*, *68*(12), 1723–1727. DOI: 10.1021/np040239j.

Le, T.-K.-D., Duong, T.-H., Nguyen, H. T., Pham, N.-K.-T., Vo, T.-P.-G., Nguyen, N.-H., Niamnont, N., Sichaem, J. & Tran, T.-M.-D. (2024). Antimicrobial sesquiterpenes from the cultured mycobiont *Diorygma pruinosum* against methicillin-resistant *Staphylococcus aureus* isolated from Vietnamese street foods. *RSC Advances*, *14*(7), 4871–4879. DOI: 10.1039/D3RA07112J.

Le, D. H., Takenaka, Y., Hamada, N. & Tanahashi, T. (2013). Eremophilane-type sesquiterpenes from cultured lichen mycobionts of *Sarcographa tricosa*. *Phytochemistry, Meinhart H. Zenk Memorial Issue*, *91*, 242–248. DOI: 10.1016/j.phytochem.2012.01.009.

Lucking, R., Hodkinson, B. P. & Leavitt, S. D. (2016). The 2016 classification of lichenized fungi in the Ascomycota and Basidiomycota–Approaching one thousand genera. *The Bryologist*, *119*(4), 361–416. DOI: 10.1639/0007-2745-119.4.361.

Ma, Y., Li, J., Huang, M., Liu, L., Wang, J. & Lin, Y. (2015). Six new polyketide decalin compounds from mangrove endophytic

fungus penicillium aurantiogriseum 328#. *Marine Drugs*, *13*(10), 6306–6318. DOI: 10.3390/md13106306.

Madhavi Sastry, G., Adzhigirey, M., Day, T., Annabhimoju, R. & Sherman, W. (2013). Protein and ligand preparation: Parameters, protocols, and influence on virtual screening enrichments. *Journal of Computer-Aided Molecular Design*, *27*(3), 221–234. DOI: 10.1007/s10822-013-9644-8.

Mali, R. S., Jagtap, P. G., Patil, S. R. & Pawar, P. N. (1993). Novel $AlCl_3$ catalysed syntheses of naturally occurring (±) 8-hydroxy-3-methyl-3,4-dihydroisocoumarins. *Journal of the Chemical Society, Chemical Communications*, 883–884. DOI: 10.1039/C39920000883.

Miyagawa, H., Hamada, N., Sato, M. & Eeno, T. (1994). Pigments from the cultured lichen mycobionts of *Graphis scripta* and *G. desquamescens*. *Phytochemistry, The International Journal of Plant Biochemistry*, *36*(5), 1319–1322. DOI: 10.1016/S0031-9422(00)89659-4.

Ngoc Mai, T. T., Minh, P. N., Phat, N. T., Chi, M. T., Duong, T. H., Nhi Phan, N. H., Minh An, T. N., Dang, V.-S., Van Hue, N., Hong Anh, N. T. & Tri, M. D. (2024). *In vitro* and *in silico* docking and molecular dynamic of antimicrobial activities, alpha-glucosidase, and anti-inflammatory activity of compounds from the aerial parts of *Mussaenda saigonensis*. *RSC Advances*, *14*(17), 12081–12095. DOI: 10.1039/D4RA01865F.

Ortiz, A., Castro, M. & Sansinenea, E. (2019). 3,4-Dihydroisocoumarins, interesting natural products: Isolation, organic syntheses and biological activities. *Current Organic Synthesis*, *16*(1), 112–129. DOI: 10.2174/1570179415666180924123439.

Rosabal, D. & Pino-Bodas, R. (2024). A review of laboratory requirements to culture Lichen Mycobiont species. *Journal of Fungi*, *10*(9), 9. DOI: 10.3390/jof10090621.

Satapathy, K., Pradhan, S. & Upreti, D. K. (2021). *Addition of 96 Lichen Species to the state of Odisha from Similipal Biosphere Reserve*. DOI: 10.3897/arphapreprints.e65955.

Singh, K. P., Singh, P. & Sinha, G. P. (2018). Lichen diversity in the Eastern Himalaya biodiversity hotspot region, India. *Cryptogam Biodiversity and Assessment*, (01). DOI: 10.21756/cab.esp9.

Srinivasan, M., Shanmugam, K., Kedike, B., Narayanan, S., Shanmugam, S. & Gopalasamudram Neelakantan, H. (2020). Trypethelone and phenalenone derivatives isolated from the mycobiont culture of *Trypethelium eluteriae* Spreng. And their anti-mycobacterial properties. *Natural Product Research*, *34*(23), 3320–3327. DOI: 10.1080/14786419.2019.1566823.

Sukandar, E. R., Kaennakam, S., Wongsuwan, S., Chatwichien, J., Krobthong, S., Yingchutrakul, Y., Mahatnirunkul, T., Mulya, F., Parasuk, V., Harding, D. J., Poldorn, P., Rungrotmongkol, T., Tip-pyang, S., Aonbangkhen, C. & Chavasiri, W. (2023). Schomburginones A–J, geranylated benzophenones from the leaves of *Garcinia schomburgkiana* and their cytotoxic and anti-inflammatory activities. *Phytochemistry*, *211*, 113701. DOI: 10.1016/j.phytochem.2023.113701.

Sun, Y.-Z., Kurtán, T., Mándi, A., Tang, H., Chou, Y., Soong, K., Su, L., Sun, P., Zhuang, C.-L. & Zhang, W. (2017). Immunomodulatory polyketides from a phoma-like fungus isolated from a soft coral. *Journal of Natural Products*, *80*(11), 2930–2940. DOI: 10.1021/acs.jnatprod.7b00463.

Sun, Y., Liu, Y., Jiang, P., Wang, S.-Y., Pan, J., Guan, W., Wang, Y.-X., Kuang, H.-X., Wang, Y.-H. & Yang, B.-Y. (2025). A new 3,4-dihydroisocoumarin and an antiinflammatory coumarin from the roots of *Saposhnikovia divaricata* (Turcz.) Schischk. *Natural Product Research*, *39*(15), 4229–4238. DOI: 10.1080/14786419.2024.2334317.

Sun, L. Y., Liu, Z. L., Zhang, T., Niu, S. B. & Zhao, Z. T. (2010). Three antibacterial naphthoquinone analogues from cultured mycobiont of lichen *Astrothelium* sp. *Chinese Chemical Letters*, *21*(7), 842–845. DOI: 10.1016/j.cclet.2010.03.024.

Takenaka, Y., Hamada, N. & Tanahashi, T. (2005). Monomeric and dimeric dibenzofurans from cultured mycobionts of *Lecanora iseana*. *Phytochemistry, Reports on Structure Elucidation*, *66*(6), 665–668. DOI: 10.1016/j.phytochem.2004.12.031.

Takenaka, Y., Naito, Y., Le, D. H., Hamada, N. & Tanahashi, T. (2013). Naphthoquinones and phenalenone derivatives from the cultured lichen mycobionts of Trypethelium sp. *Heterocycles*, *87*(9), 1897–1902. DOI: 10.3987/com-13-12768.

Tammam, M. A., Gamal El-Din, M. I., Abood, A. & El-Demerdash, A. (2023). Recent advances in the discovery, biosynthesis, and therapeutic potential of isocoumarins derived from fungi: A comprehensive update. *RSC Advances*, *13*(12), 8049–8089. DOI: 10.1039/D2RA08245D.

Tanahashi, T., Takenaka, Y., Nagakura, N. & Hamada, N. (2003). 6H-Dibenzo[b,d]pyran-6-one derivatives from the cultured lichen mycobionts of *Graphis* spp. and their biosynthetic origin. *Phytochemistry*, *62*(1), 71–75. DOI: 10.1016/S0031-9422(02)00402-8.

Tran, T.-M.-D., Aonbangkhen, C., Duong, T.-H., Nguyen, T.-H.-M., Ho, M.-T.-T., Chavasiri, W., Wongsuwan, S., Chatwichien, J., Giao Vo, T.-P., Nguyen, N.-H., Kiriwan, D. & Choowongkomon, K. (2024). Diphenyl ethers from the cultured lichen mycobiont of *Graphis handelii* Zahlbr. *Heliyon*, *10*(4), e25763. DOI: 10.1016/j.heliyon.2024.e25763.

Tsukamoto, S., Miura, S., Yamashita, Y. & Ohta, T. (2004a). Aspermytin A: A new neurotrophic polyketide isolated from a marine-derived fungus of the genus *Aspergillus*. *Bioorganic & Medicinal Chemistry Letters*, *14*(2), 417–420. DOI: 10.1016/j.bmcl.2003.10.053.

Tsukamoto, S., Miura, S., Yamashita, Y. & Ohta, T. (2004b). Aspermytin A: A new neurotrophic polyketide isolated from a marine-derived fungus of the genus *Aspergillus*. *Bioorganic & Medicinal Chemistry Letters*, *14*, 417–420. DOI: 10.1002/chin.200419213.

Yang, J. X., Chen, Y., Huang, C., She, Z. & Lin, Y. (2011). A new isochroman derivative from the marine fungus Phomopsis Sp. (No. ZH-111). *Chemistry of Natural Compounds*, *47*(1), 15–17. DOI: 10.1007/s10600-011-9820-9.

Yasmin, F. & Jabin, R. (2024). Physiology of lichen. In *Chemistry, biology and pharmacology of lichen* (pp. 71–80), John Wiley & Sons, Ltd. DOI: 10.1002/9781394190706.ch6.